Technical Note

1970-30

Processing a Partially Coherent Large Seismic Array for Discrimination

R. T. Lacoss
G. T. Kuster

27 November 1970

Prepared for the Advanced Research Projects Agency
under Electronic Systems Division Contract F19628-70-C-0230 by

Lincoln Laboratory

MASSACHUSETTS INSTITUTE OF TECHNOLOGY

Lexington, Massachusetts

MASSACHUSETTS INSTITUTE OF TECHNOLOGY

LINCOLN LABORATORY

PROCESSING A PARTIALLY COHERENT LARGE SEISMIC ARRAY FOR DISCRIMINATION

R. T. LACOSS
G. T. KUSTER

Group 22

TECHNICAL NOTE 1970-30

27 NOVEMBER 1970

LEXINGTON MASSACHUSETTS

The work reported in this document was performed at Lincoln Laboratory, a center for research operated by Massachusetts Institute of Technology. This research is a part of Project Vela Uniform, which is sponsored by the Advanced Research Projects Agency of the Department of Defense under Air Force Contract F19628-70-C-0230 (ARPA Order 512).

ABSTRACT

A stochastic model has been proposed to characterize the teleseismic short period P-wave signal variations observed within a Large Aperture Seismic Array (LASA). The model asserts that, in the frequency domain, the received signal is equal to some average signal multiplied by a random gain and phase. Within a Montana LASA subarray the mean value of the modulus squared of the random term can be roughly approximated by $1 + 0.18f^2$, where f is frequency. For sensors drawn from the full LASA aperture the value is approximated by $1 + 2.0f^2$.

An incoherent signal processing method, spectraforming, is introduced as a viable alternative to beamforming for obtaining spectral information at frequencies above about 1.0 Hz. The spectraform is essentially the average power in sensors with a correction subtracted for background noise power contributions. It is demonstrated that although beamforming will give more noise rejection than spectraforming the latter can be superior in terms of output signal to noise ratio when input signal variations between sensors are large.

Expressions have been obtained for the signal power spectral density expected from various modes of processing. Spectra from subarray beams and sums, spectra from array beams and beams of subarray sums, and spectraforms are all considered. Results show for example that the event power output from spectraforming, beamforming of individual sensors, and beamforming of subarray sums will decrease in that order. In the case of actual events considered, the amounts of loss at 3.0 Hz, relative to spectraforming, are about 10 and 20 dB respectively.

Accepted for the Air Force
Joseph R. Waterman, Lt. Col., USAF
Chief, Lincoln Laboratory Project Office

I. INTRODUCTION

We wish to discuss certain signal properties and signal processing capabilities of large arrays of seismometers. The emphasis is upon short period vertical instruments and teleseismic P-wave signals although some of the concepts used can be utilized in other situations. Figure 1 is a schematic diagram of an array, the earth structure near the array, and the incident signal. The array has been shown as a collection of small subarrays since this is the configuration of the Large Aperture Seismic Array (LASA) in Montana and of the array currently under construction in Norway (NORSAR). Typically, the separation of instruments within a subarray is considerably less than that between subarrays.

Each sensor of any seismic array will contain seismic and instrumental noise as well as output generated by the incident signal of interest. For the present we assume the signal is sufficiently large so that the background noise can be neglected. However, even with no background noise, the signals at different sensors are not identical. One possible model for this phenomena is suggested by Figure 1. Suppose that at some reference plane beneath the array there is incident a plane wave with slowness $\underline{\alpha}$. The motion at position $\underline{r}$ in that plane is $s(t - \underline{\alpha}\cdot\underline{r})$ where $\underline{\alpha}\cdot\underline{r}$ is the dot product of slowness and position. The output of the m^{th} sensor of the n^{th} subarray is not $s(t - \underline{\alpha}\cdot\underline{r}_{mn})$. One can imagine that the signal at sensor mn is obtained from $s(t - \underline{\alpha}\cdot\underline{r}_{mn})$ by a cascade of three linear filters. The first filter is a pure time delay, τ_{mn}. The second filter is common to all sensors and represents the average change in waveform between the reference plane and the surface. The final filter represents perturbations which are specific to the particular sensor. Let $S_{mn}(f)$ be the Fourier transform of the signal at sensor mn after a time shift of $\underline{\alpha}\cdot\underline{r}_{mn} + \tau_{mn}$. We then have

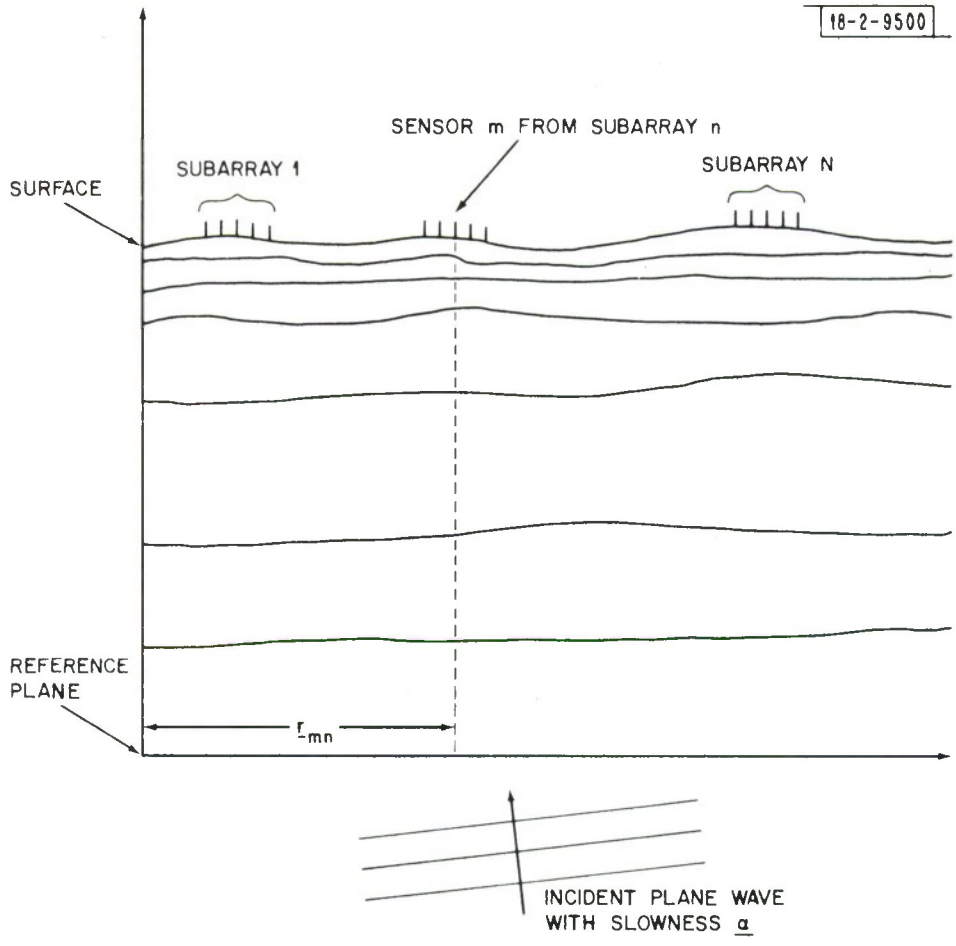

Fig. 1. Schematic of body wave incident upon a large seismic array.

$$S_{mn}(f) = S(f)T(f)\{1 + \mathcal{H}_{mn}(f)\} \quad (1)$$

where S(f) is the transform of s(t), T is the average waveform change, and $\mathcal{H}_{mn}(f)$ represents perturbations. The $\mathcal{H}_{mn}$ cause the received signal to be only partially coherent across the array.

The perturbations $\mathcal{H}_{mn}(f)$ are due to fixed deterministic variations in earth structure and in that sense are not random. However, it is generally quite impossible to predict the $\mathcal{H}_{mn}$ and we will find it convenient to consider them to be random variables with zero expected value. In general the $\mathcal{H}_{mn}$ are not independent of each other. For example, signals observed within one of the LASA subarrays are more similar to each other than to signals drawn from other, more distant, subarrays. One way to model this phenomenon is to assume that the correlation between the $\mathcal{H}_{mn}$ is some decreasing function of the distance between the sensors involved. Rather than consider this general case we have selected to model the situation in a way which is somewhat simpler and which uses the organization of large arrays into an array of subarrays. Specifically one can expand $S_{mn}(f)$ as

$$S_{mn}(f) = S(f)T(f)\{1 + H_{mn}(f)\}\{1 + H_n(f)\} \quad (2)$$

where the perturbation has been factored into two components. The factors $1 + H_n$ account for gross differences between subarrays and the $1 + H_{mn}$ for differences within the subarray. This is the model we shall use with the assumption that both the real and imaginary parts of all of the different H_{mn} and H_n are uncorrelated and zero mean. We also define

$$E\, H_{mn}(f)H^*_{mn}(f) = 2\sigma^2(f), \tag{3}$$

$$E\, H_n(f)H_n(f) = 2\sigma_A^2(f) \tag{4}$$

and

$$E\, H_{mn}(f)H^*_{mn}(f) = 2\sigma_S^2(f) \tag{5}$$

where E denotes mathematical expectation.

The variety of different spectra which can be obtained from a large array is very great and it is important to understand their properties. The following are three quantities which might be of interest in the absence of additive background noise.

1. P(M,N,f): Arithmetic mean power at frequency f of M sensors from each of N subarrays. Thus, suppressing the explicit dependence on frequency,

$$P(M,N) = \frac{1}{MN} \sum_{n=1}^{N} \sum_{m=1}^{M} |S_{mn}|^2 \tag{6}$$

2. $P_B(M,N,f)$: Power on a beam formed from M sensors from each of N subarrays. That is,

$$P_B(M,N) = S_B(M,N)S_B^*(M,N) \tag{7}$$

where

$$S_B(M,N) = \frac{1}{MN} \sum_{n=1}^{N} \sum_{m=1}^{M} S_{mn} \tag{8}$$

is the beam.

3. $P_{SB}(M,N,f)$: Power of a beam formed from straight sum traces from N subarrays. The sum trace is the average of the waveforms from M instruments in

a subarray. In order to obtain an expression for this quantity we assume that $\underline{\alpha}\cdot\underline{r}_{mn} + \tau_{mn} = \tau_n + \underline{\alpha}\cdot\underline{\Delta r}_{mn}$ where τ_n is the delay used for beamforming the sums and $\underline{\Delta r}_{mn}$ is the location of sensor mn relative to the center of subarray n. Using this we have

$$P_{SB}(M,N,f) = S_{SB}(M,N)S^*_{SB}(M,N) \tag{9}$$

where

$$S_{SB}(M,N) = \frac{1}{MN}\sum_{n=1}^{N}\sum_{m=1}^{M} S_{mn}e^{-i2\pi f(\underline{\alpha}\cdot\underline{\Delta r}_{mn})} \tag{10}$$

is the beam of subarray sums.

Each of these quantities is a random variable. In this report we obtain and utilize the mathematical expected value of all of these random variables.

Although they must ultimately be considered, the distributions and/or higher moments of P, P_{SB}, and P_B are not given in this report. We simply insert here a brief discussion concerning such distributions and point out the similarities between the seismic problem and other more common research problems. In the body of this report we use only first and second moments of the H_n, etc., and have used no assumptions or relationships which are inconsistent with the most likely distributions which might be assumed in the future.

It seems reasonable to assume that the H_{mn} and H_n are caused by random inhomogeneities in the earth beneath the array. In fact one might attribute the H_n to relatively deep structure and H_{mn} to local structure beneath the different subarrays. In this case the model of $1 + H_{mn}$ as a cascade of two filters with gain functions $1 + H_n$ and $1 + H_{mn}$ is physically meaningful. Assuming the H_n and H_{mn} are caused by similar phenomena it would seem that they should have similar probability distributions.

However the $1 + \mathcal{H}_{mn}$ are also caused by the same phenomena and should in some sense also have the same distribution. This excludes many possible distributions which might be analytically convenient. For example, the $1 + H_n$ cannot be Gaussian random variables. However they can be log normal. That is if the log $(1 + H_n)$, etc., are complex normal distributions then the requirement that all the distribution be similar can be satisfied. Of course, other distributions do exist. In a sense, similar considerations have led to the use of the log normal distribution in models of propagation through other random media. For example, the propagation of laser beams through the atmosphere and sound through the ocean under some conditions lead to these log normal distributions.

One might simplify the analysis by making other assumptions concerning the $\mathcal{H}_{mn}$. For example, suppose they are in fact Gaussian and that we consider $1 + \mathcal{H}_{mn} = 1 + H_n + H_{mn}$ rather than the factored form assumed above. In this case the Gaussian assumption is quite satisfactory. However, there is no obvious physical line of reasoning which would lead to this situation where effects are additive.

It is a relatively simple matter to introduce additive instrument and seismic background noise into our model. In general such noise can be correlated between instruments. However, it is now current practice to separate instruments sufficiently so that such correlation is minimal at least at 1 Hz and above. Thus we shall deal only with noise which is independent between sensors. This in fact makes certain aspects of the analysis tractable which otherwise would not be. We will consider the additive noise only in a later part of this report when we evaluate the relative efficiency of various signal processing methods for discrimination between earthquakes and explosions. For the present we continue with a model which contains no such noise to obscure observations.

II. EXPECTED POWER FROM BEAMS, BEAMS OF SUMS AND SENSORS

The mathematical expected value of P(M,N) is the same as that of $|S_{mn}|^2$. Thus we immediately obtain

$$E\{P(M,N)|S,T\} = |ST|^2 E\{|1+\mathcal{H}_{mn}|^2\}$$

$$= |ST|^2 (1+2\sigma^2). \tag{11}$$

It is assumed that S and T are constants and that the expectation is conditioned upon them. Using the alternative expression of equation (2) for S_{mn} gives

$$E\{P(M,N)|S,T\} = |ST|^2 (1+2\sigma_A^2)(1+2\sigma_S^2). \tag{12}$$

Finally if a single subarray is considered and H_n as well as S, T is assumed known we have

$$E\{P(M,1)|S,T,H_n\} = |ST(1+H_n)|^2 (1+2\sigma_S^2). \tag{13}$$

The expected value of $P_{SB}(M,N)$ is slightly more difficult to obtain. We first consider $P_{SB}(M,1)$ with S, T and H_n all given. In this case

$$P_{SB}(M,1) = \frac{|ST(1+H_n)|^2}{M^2} \left| \sum_{m=1}^{M} [(1+H_{mn}) e^{-i2\pi f(\underline{\alpha}\cdot\underline{\Delta r}_{mn})}] \right|^2 \tag{14}$$

Taking the expected value of this gives

$$E\{P_{SB}(M,1)|S,T,H_n\} = |ST(1+H_n)|^2 (B_n + \frac{2\sigma_S^2}{M}) \tag{15}$$

where

$$B_n = G_n G_n^* \tag{16}$$

and

$$G_n = \frac{1}{M} \sum_{m=1}^{M} e^{-i2\pi f(\underline{\alpha} \cdot \underline{\Delta r}_{mn})} . \tag{17}$$

If H_n and H_{mn} are independent then

$$E\{ P_{SB}(M,1) \mid S,T,n\} = |ST|^2 (1 + 2\sigma_A{}^2) (B_n + \frac{2\sigma_S{}^2}{M}) \tag{18}$$

This expectation is conditioned on n only because the geometry of subarrays may vary and this will result in different B_n. If $P_{SB}(M,1)$ is averaged over N subarrays then we get

$$E\{ P_{SB}(M,1) \mid S,T\} = |ST|^2 (1 + 2\sigma_A{}^2) (\overline{B} + \frac{2\sigma_S{}^2}{M}) \tag{19}$$

where

$$\overline{B} = \frac{1}{N} \sum_{n=1}^{N} B_N \tag{20}$$

The complete expectation of $P_{SB}(M,N)$ is obtained as follows. By substituting equation (2) into (10), (10) into (9), and taking expected values we obtain

$$E\{ P_{SB}(M,N) \mid S,T\} = \frac{|ST|^2}{(NM)^2} \sum_{j,k=1}^{N} \sum_{\ell,m=1}^{M} \{ (1 + 2\sigma_A{}^2 \delta_{jk})$$

$$(e^{-i2\pi f(\underline{\alpha} \cdot (\underline{\Delta r}_{\ell j} - \underline{\Delta r}_{mk}))}) (1 + 2\sigma_S{}^2 \delta_{jk} \delta_{\ell m})\} \tag{21}$$

where δ_{jk} is the Kroneker delta. This is considerably simplified by using definitions (16), (17) and (19) above as well as

$$B = \left| \frac{1}{NM} \sum_{n=1}^{N} \sum_{m=1}^{M} e^{-i2\pi f(\underline{\alpha} \cdot \underline{\Delta r}_{mn})} \right|^2 . \tag{22}$$

This gives

$$E\{P_{SB}(M,N)\,|\,S,T\} = |ST|^2[B + \frac{2\sigma_A^2}{N}\,\overline{B} + \frac{2\sigma_S^2(1+2\sigma_A^2)}{MN}]. \tag{23}$$

Both B and $\overline{B}$ in equation (22) are subarray beam pattern effects. B is the squared magnitude of the average complex gain of the subarrays and $\overline{B}$ is the average of the squared magnitudes of the individual subarray gains. If all subarrays are identical then $B = \overline{B}$.

Expected values for $P_B(M,N)$ are obtained by putting $B_n = B = 1$ in all the expressions for $\{P_{SB}(M,N)\}$. Thus

$$E\{P_B(M,1)\,|\,S,T,H_n\} = |ST(1+H_n)|^2\,(1 + \frac{2\sigma_S^2}{M}), \tag{24}$$

$$E\{P_B(M,1)\,|\,S,T\} = |ST|^2\,(1+2\sigma_A^2)\,(1 + \frac{2\sigma_S^2}{M}), \tag{25}$$

and

$$E\{P_B(M,N)\,|\,S,T\} = |ST|^2\,[1 + \frac{2\sigma_A^2}{N} + \frac{2\sigma_S^2(1+2\sigma_A^2)}{MN}]. \tag{26}$$

III. ESTIMATION OF σ^2, σ_S^2 AND σ_A^2.

One way to estimate the subarray signal variation parameter σ_S^2 is to compare average power from sensors with average power from subarray beams. From equations (11) and (25) one would expect the ratio to be

$$\frac{E\{P(M,N) \mid S,T\}}{E\{P_B(M,1) \mid S,T\}} = (1 + 2\sigma_S^2) / (1 + \frac{2\sigma_S^2}{M}) \qquad (27)$$

Figure 2 shows a plot of observations of $P(M,N)/P_B(M,1)$ as measured using from 9 to 12 sensors per subarray for 5 subarrays in LASA. Thus $P(M,N)$ is the average power from about 50 sensors and the $P_B(M,1)$ used was the average power of five subarray beams. The spectra were obtained using the discrete Fourier transform of ten seconds of data sampled twenty times per second. Possible effects of the frequency window will be discussed subsequently. The events used were a large earthquake and a presumed underground explosion located 80 to 90 degrees from LASA. The events are sufficiently large so that background seismic and instrument noise can be neglected.

If the H_{mn} are caused by random inhomogeneities in the earth then the behavior of σ_S^2 as a function of frequency must depend upon the statistical properties of these inhomogeneities. There must be basic parameters such as characteristic size, perhaps normalized by wavelength, which determine the behavior of σ_S^2 as a function of frequency. The same is true for σ_A^2. We have not yet investigated this area. We have simply chosen to assume that $\sigma_S^2(f) = (C_S f)^2$. Such an assumption appears to fit the data reasonably well but we have not yet attached any physical significance to the constant C_S. It may well be that some other function of frequency would give just as good a fit and have a better physical or theoretical basis.

Figure 2 shows theoretical values of $E\{P(M,N)|S,T\}/E\{P_B(M,1)|S,T\}$ for M=10 and several values of C_S. It appears that C_S in the range 0.3 to 0.4 gives a reasonable fit to the data. The effect of different numbers of sensors in each subarray is small and the typical number 10 has been used.

The variable $\sigma^2 = E(H_{mn} H^*_{mn})$ can be estimated using one element from each subarray of LASA. The ratio of expected average power to expected beam power, obtained from equations (11) and (26) and using the relationship

$$\sigma^2 = \sigma_A^2 + \sigma_S^2 + 2\sigma_A^2\sigma_S^2 \ , \tag{28}$$

is

$$\frac{E\{P(1,N)|S,T\}}{E\{P_B(1,N)|S,T\}} = \frac{1+2\sigma^2}{1+\frac{2\sigma^2}{N}} \ . \tag{29}$$

As one might expect this is functionally the same as for choosing instruments from within a single subarray. An array of one instrument per subarray acts as a large subarray. The ratio $P(1,N)/P_B(1,N)$ has been calculated from a large bomb and earthquake. The powers, P, used were in both cases the average obtained using two different sets of 21 sensors from LASA. The data are shown in Figure 3. The scatter is large but might be reduced by considering more events or using several other sets of 21 sensors. Neither has been attempted. Also the higher moments or distribution of the P, which would help to evaluate the scatter, have not been obtained at this time.

An estimate of $\sigma^2(f)$ could be obtained from each point on Figure 3. At each frequency such estimates might be combined to obtain a final estimate of σ^2. We have chosen not to do this but to assume that $\sigma^2(f)$, like $\sigma_S^2(f)$, is quadratic in frequency. The theoretical curves on Figure 3 are given by equation (29) with $\sigma^2(f) = (Cf)^2$. For

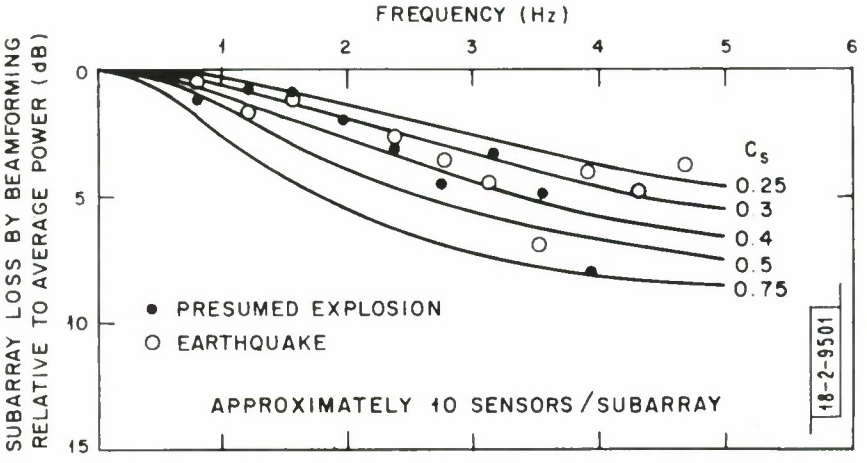

Fig. 2. Subarray power loss by beamforming relative to a single sensor vs frequency. Theoretical curves shown for $\sigma_S^2 = C^2_S f^2$.

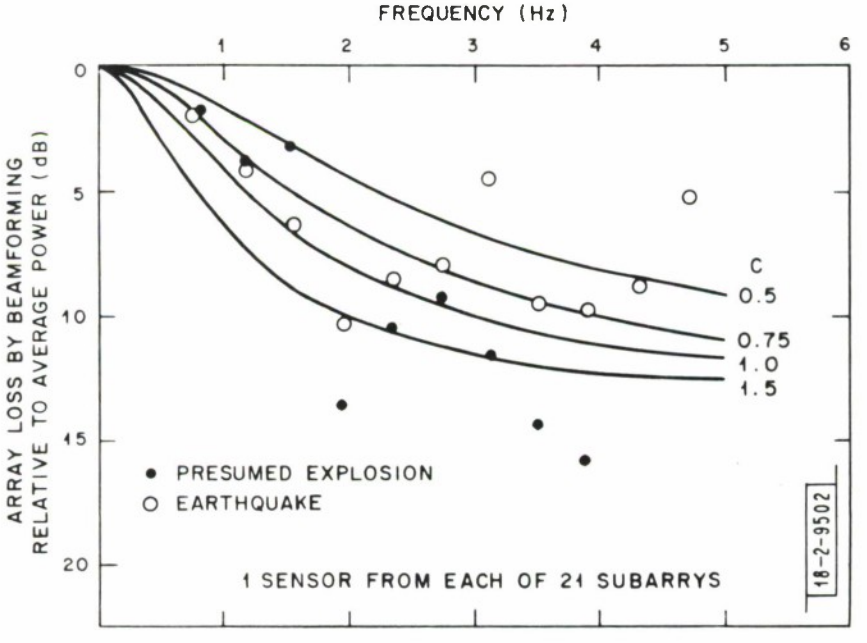

Fig. 3. Array loss by beamforming relative to a single sensor vs frequency. Theoretical curves shown for $\sigma^2 = C^2 f^2$.

the purpose of continuing discussion of a specific situation we have chosen C = 1.0 to be a good fit to the data. It should be noted that if $(Cf)^2$ is considerably larger than unity that the signal is almost incoherent and beamforming will give almost 1/N reduction in signal power.

If σ^2 and σ_S^2 are quadratic in frequency as assumed above then

$$\sigma_A^2 = (C^2 - C_S^2)f^2 / (1 + 2C_S^2 f^2) . \tag{30}$$

Thus σ_A^2 is approximately quadratic in frequency only if $2C_S^2 f^2 < 1$. Roughly this makes σ_A^2 quadratic only up to about 2 Hz for the values of C, C_S we have estimated. This is somewhat bothersome since one might wish σ_A^2 to have a functional dependence on frequency which is the same as σ^2 and σ_S^2. This difficulty has not been resolved at this time.

IV. DISCUSSION OF RELATIVE POWER FOR SEVERAL DIFFERENT ARRAY OUTPUTS

It has often been computationally expedient to consider only direct sum signals from large arrays. The consequences of this are well known for the theoretical case of a plane wave. However, we have just seen the extent to which signals in an array are not simple plane waves. The variables σ_S^2 and σ_A^2 can be considered to characterize this phenomenon.

Consider the spectra which might be obtained from a subarray direct sum and from the individual instruments of the subarray. The ratio of the expected values of these quantities is obtained from equations (12) and (19) as

$$\frac{E\{P(M,1)\,|\,S,T\}}{E\{P_{SB}(M,1)\,|\,S,T\}} = (1 + 2\sigma_S^2)/(\bar{B} + \frac{2\sigma_S^2}{M}) \qquad (31)$$

where $\bar{B}$ is the average beam pattern effect of the subarrays used in the experiment. $\bar{B}$ would be the only effect in the case of perfect plane waves. If $\bar{B}$ is small compared to $2\sigma_S^2/M$ it is clear that the beam pattern will have little effect upon the observations.

The gain $\bar{B}$ depends upon the sensor configurations in each subarray and the slowness vector $\underline{\alpha}$ as well as frequency. Figure 4 shows the value of $-10 \log B_j$ as a function of frequency and the angles of $\underline{\alpha}$ in the first quadrant for a typical set of 12 elements in a subarray. The magnitude of $\underline{\alpha}$ has been fixed at 23 km/sec. which is close to that for both events studied in this report. The function in other quadrants can be found to a good approximation by symmetry. The function is very similar at other sites for frequency less than about three cycles. For larger frequencies the shape is somewhat similar but at half of the subarrays the pattern is rotated by about thirty degrees. The value of $\bar{B}(f)$ will certainly be less than the maximum $B_j(f)$. By using Figure 4 with an

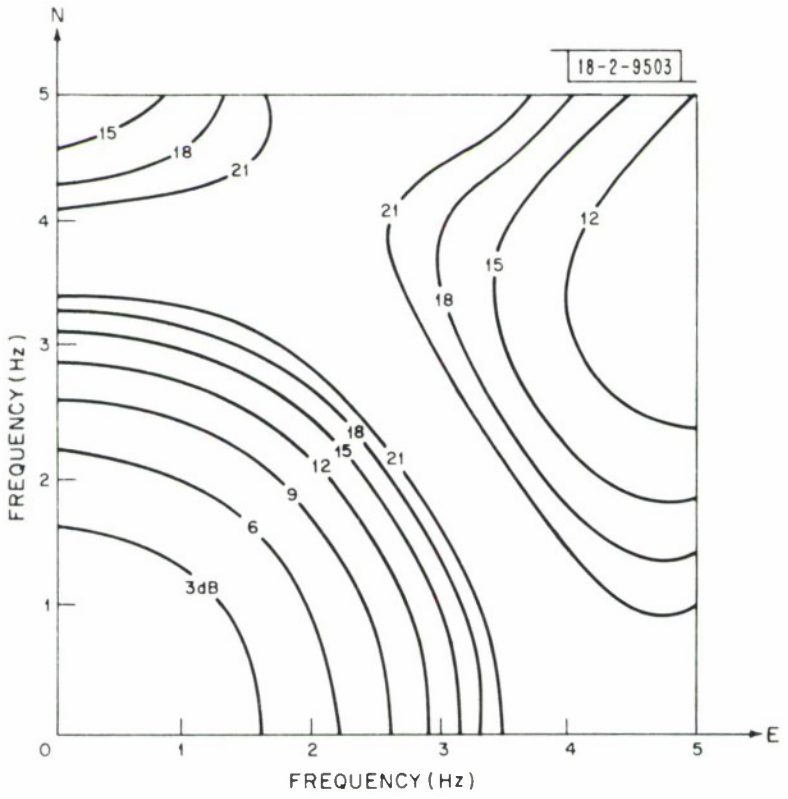

Fig. 4. Subarray straight sum attenuation of a plane wave with slowness 1/23. Attenuation shown in dB as a function of frequency and azimuth in first quadrant.

angle East from North of 60° we will be able to show that the subarray beam pattern does not significantly affect observed spectra from LASA except at low frequencies.

Figure 5 shows the average power of sensors in subarrays divided by the average power of straight sums for the two large events we have considered previously. Several theoretical curves given by equation (31) are also shown. One of these is for $\sigma_S^2 = 0$. In this case the beam pattern predicts a very sudden loss of signal in the region from three to four Hertz. This notch is not visible on the data shown and we have seen no evidence of it on any of our data. The $\sigma_S^2 = 0$ curve shown uses $B_j(f)$ as obtained from Figure 4 in a direction picked to give the least attenuation of high frequencies. Curves are also shown for $\sigma_S^2 = (0.3f)^2$ and fixed values of $\overline{B}$. It is clear that if the subarray beam predicts more than 10 db loss ($\overline{B} \leq 0.1$) then the power on the subarray straight sum is very insensitive to the true value of $\overline{B}_j$. For 10 sensor subarrays from LASA it appears that the direct sum output power is determined more by σ_S^2 than by $\overline{B}$ for frequencies greater than 2.7 Hz. It should be noted that this does depend on the value of M. Larger M would cause $\overline{B}$ to have a greater impact. However, for fixed subarray size, increasing M must reduce interelement spacing and probably result in a smaller effective σ_S^2. Finally the theoretical ratio of equation (31) is shown in Figure 5 for $C = 0.3$ and a reasonable value for $\overline{B}$, obtained from Figure 4.

Another quantity of interest might be the average power from the steered beams from subarrays. Figure 6 shows the theoretical relationship of this quantity to both individual sensor average powers and to direct sum average powers. The theoretical ratio of subarray beam powers to straight sum average powers is

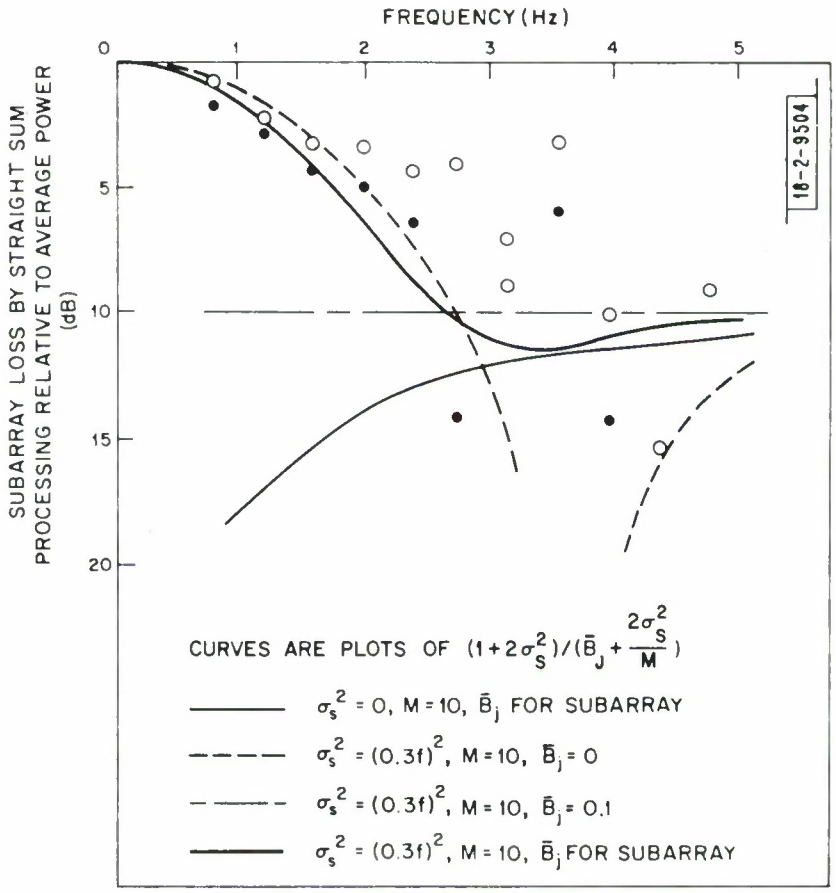

Fig. 5. Subarray loss by straight sum processing relative to single sensor vs frequency.

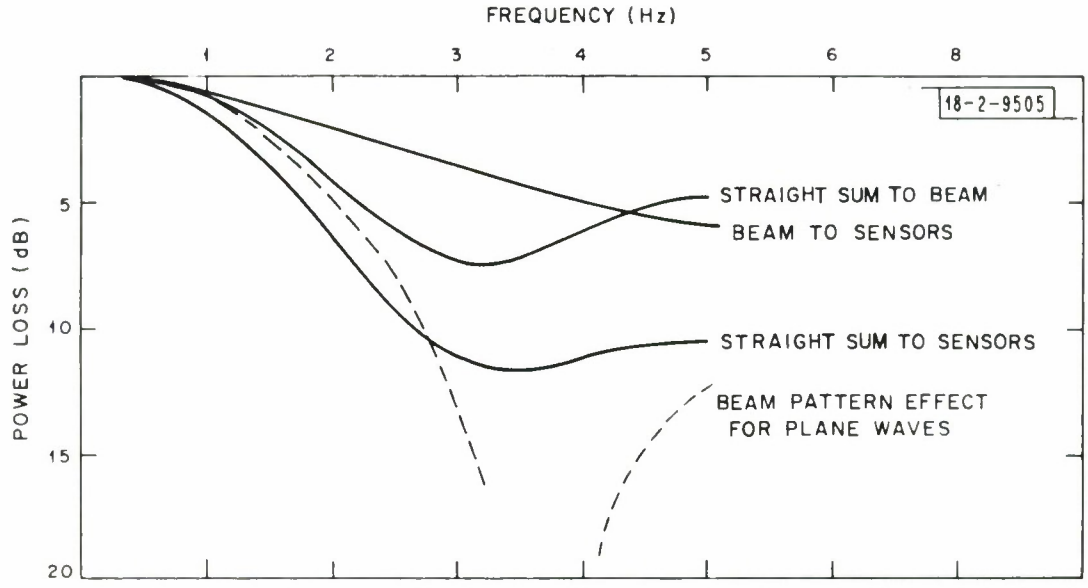

Fig. 6. Summary of various theoretical subarray power losses as a function of frequency. Slowness = 1/23, number of sensors = 10, $\sigma_S^2 = (0.3f)^2$.

$$\frac{E\{P_B(M,1)\,|\,S,T\}}{E\{P_{SB}(M,1)\,|\,S,T\}} = \left(1+\frac{2\sigma_S^2}{M}\right) \Big/ \left(\bar{B}+\frac{2\sigma_S^2}{M}\right). \tag{32}$$

which is also given by

$$\left(\frac{E\{P_B(M,1)\,|\,S,T\}}{E\{P_{SB}(M,1)\,|\,S,T\}}\right) = \left(\frac{E\{P_B(M,1)\,|\,S,T\}}{E\{P(M,1)\,|\,S,T\}}\right)\left(\frac{E\{P(M,1)\,|\,S,T\}}{E\{P_{SB}(M,1)\,|\,S,T\}}\right) \tag{33}$$

The inverse of the first term on the right is given by equation (27) and the second is given by equation (31). All three terms have been shown on a dB scale on the figure with $E\{P\}/E\{P_B\}$ used in place of $E\{P_B\}/E\{P\}$ so that all have the same sign. The beam pattern effect for perfect plane waves is also shown. If signals were plane waves then curve (1) would be at 0 dB and curves (2), (3) and (4) would coincide.

It should be clear that the model we have developed can be used to predict array performance as a function of frequency for many modes of operation. We complete this section with two more examples. First consider the power on array beams formed from subarray beams and from subarray sums. We assume that $B = \bar{B}$ and obtain the ratio

$$\frac{E\{P_B(M,N)\,|\,S,T\}}{E\{P_{SB}(M,N)\,|\,S,T\}} = \frac{1+\dfrac{2\sigma_S^2}{M}\left(\dfrac{1}{N}\;\dfrac{1+2\sigma_A^2}{\dfrac{1+2\sigma_A^2}{N}}\right)}{\bar{B}+\dfrac{2\sigma_S^2}{M}\left(\dfrac{1}{N}\;\dfrac{1+2\sigma_A^2}{\dfrac{1+2\sigma_A^2}{N}}\right)} \tag{34}$$

from equations (23) and (26). Observe that this is the same as equation (32) but with

$2\sigma_S^2/M$ multiplied by the array quantity $(1 + 2\sigma_A^2) / (N (1 + 2\sigma_A^2/N))$. This multiplicative factor is always between 1/N and 1. Thus this comparison will tend to make the subarray beam pattern effect somewhat stronger than when powers are compared without beamforming. Of course this neglects any questions of statistical stability. If $\sigma_A^2 = 0$ then the multiplicative factor is 1/N and the reduction of the effective $2\sigma_S^2/M$ is greatest. Figure 7 shows equation (34) for the case M = 10, N = 21, C = 1.0, C_S = 0.3, and the nominal $\overline{B}$ we have used previously. The value is controlled more by σ_S^2 and σ_A^2 than by $\overline{B}$ for f > 2.7 Hz. Note also that the curve does follow the beam pattern of a subarray for somewhat higher frequencies than does equation (32) shown on Figure 6.

Finally we wish to consider the ratio of single sensor average power to the average power of a full array beam using M sensors from each of N subarrays. This ratio, obtained from equations (11) and (26), can be written as

$$\frac{E\{P(M,N) \mid S,T\}}{E\{P_B(M,N) \mid S,T\}} = \left(\frac{1 + 2\sigma_A^2}{\frac{1 + 2\sigma_A^2}{N}} \right) \left(\frac{1 + 2\sigma_S^2}{\frac{1 + 2\sigma_S^2}{M'}} \right) \tag{35}$$

where

$$M' = M \left(\frac{N (1 + \frac{2\sigma_A^2}{N})}{1 + 2\sigma_A^2} \right) . \tag{36}$$

The first factor is that which would be obtained with $\sigma_S^2 = 0$. The second is due to the subarray but M has been increased to M'. If $\sigma_A^2 = 0$ then M' = M. Equation (35) is shown on Figure 7 for the same parameter values as equation (34). The sum of these two would give the dB relationship between the power on a beam formed from direct subarray sums and the average power on the individual instruments.

If there were any additive noise the use of 210 sensors (10 from each of 21 subarrays) would give about 23 dB of noise attenuation by beamforming. Thus, it appears that beamforming of subarray straight sums would give no improvement in signal to noise ratio for frequencies above 3 Hz since the signal power on the beam would be down a similar amount from the average signal power on individual sensors. This observation is elaborated upon in a later section where both the mean and variance of observations on the presence of noise are considered in detail.

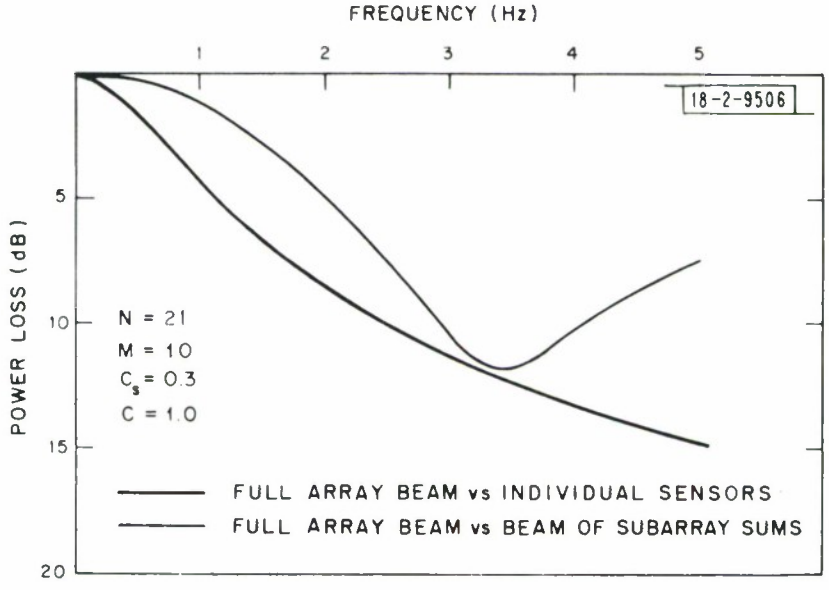

Fig. 7. Loss of beam of 21 × 10 sensors relative to single sensor and of beam of 21 subarray sums of 10 sensors relative to beam of 21 × 10 sensors vs frequency.

V. IMPACT OF USING SAMPLED DATA AND TRUNCATED SIGNALS

All of the theoretical expressions of the preceding sections assume we are dealing with the true spectra of continuous time functions. In fact the short period data from large arrays is sampled, typically at 10 or 20 times per second, and only a finite interval of time is used to estimate spectra. Sampling will introduce no fundamental difficulty so long as the data are band limited to the Nyquist interval. All the data we have used were sampled at 20 times per second giving a Nyquist interval of ±10 Hz. The data are sharply low pass filtered with a corner at 5 Hz before sampling so that we need not consider this problem. However, the effect of using finite data intervals must be considered in somewhat more detail before we can conclude that it is not truly significant. Figure 8 shows typical data and intervals used for computing transforms.

Suppose that x(t) is the waveform under consideration and that it has a Fourier transform X(f). Let h(t) be a series of unit Dirac impulse functions located every Δt seconds in the interval which is to be used to estimate X(f). All of our data is for $\Delta t = 0.05$. The transform of h(t) is H(f). Let the data interval contain p impulses and, with no loss of generality, assume the first impulse is located at $t = -\Delta t(p-1)/2$. In this case

$$H(f) = \int_{-\infty}^{\infty} h(t)e^{-i2\pi ft}dt = \frac{\sin \pi fp\Delta t}{\sin \pi f\Delta t} \quad . \tag{37}$$

The transform which can be calculated is that of the product x(t)h(t). It is true in general that the transform of a product is the convolution of the transforms. Thus

$$\hat{X}(f) = \int_{-\infty}^{\infty} X(\nu)H(f-\nu)d\nu \tag{38}$$

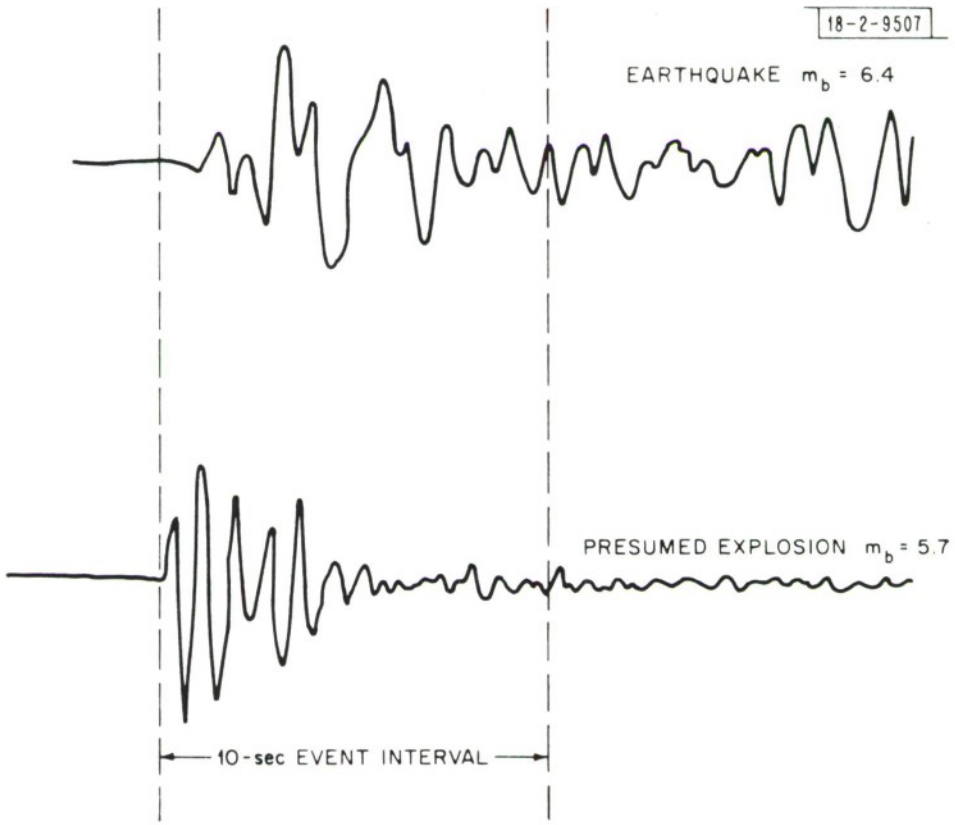

Fig. 8. Examples of data intervals used to compute spectra. Signals are subarray F4 straight sums each normalized to peak values.

is the measured quantity. The observation at f is a sum of contributions from all frequencies. The observed power, $|\hat{X}(f)|^2$, is of course the squared magnitude of such a sum.

One would want H(f) to be a very peaked function around f = 0. In that case $\hat{X}(f)$ is just a very local average of X(f). However, this may not be the case if H(f) does not go to zero quickly enough. This can be particularly troublesome if there is a region of frequencies where X(f) tends to be very large and one is attempting to measure X(f) in a region where it is very small. Figure 9 shows results from an experiment designed to demonstrate that this latter phenomena has not significantly altered our data. The figure shows average spectra from 21 subarray direct sums before and after filtering with a Butterworth filter with 3 dB corners at 3 Hz and 6 Hz. It is clear that in the 3 to 6 Hz range the spectra before and after are nearly identical. This shows that in that band, even before filtering, no significant amount of observed power was introduced from lower frequency regions via the mechanism of equation (38) although the power in those regions is large.

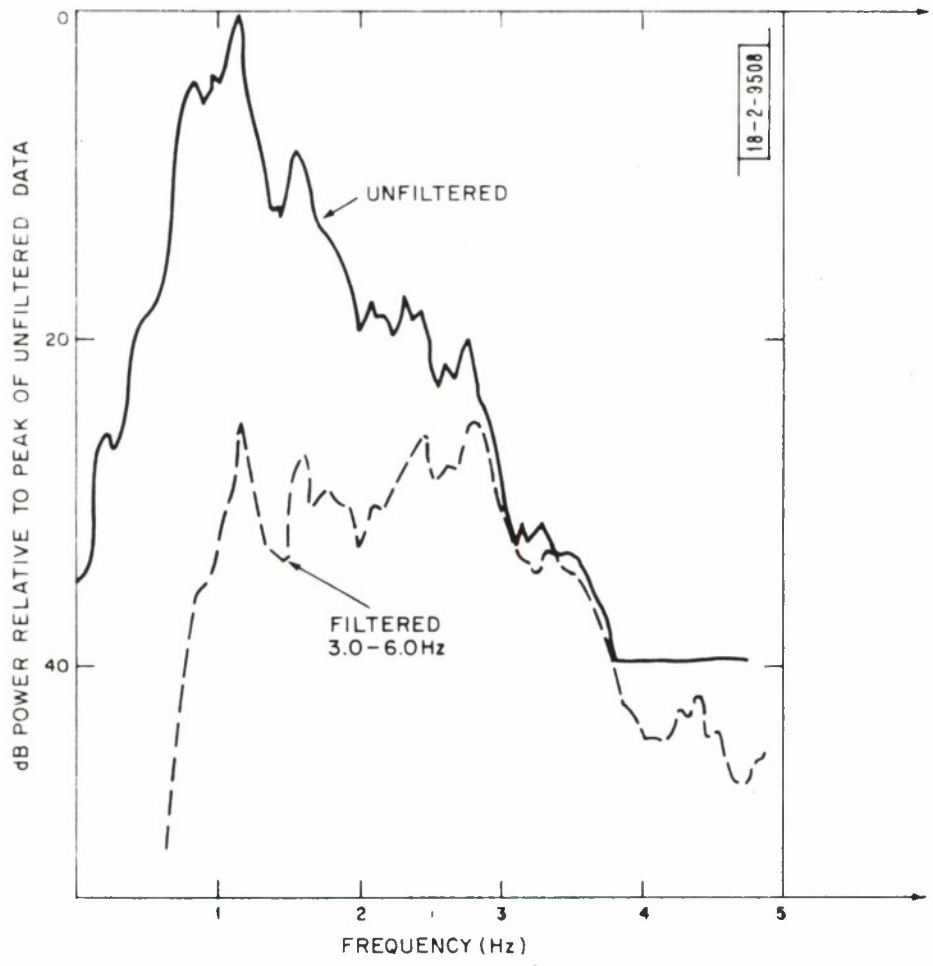

(a) Presumed explosion.

Fig. 9. Average power of 21 sensors before and after band pass filtering to 3.0 - 6.0 Hz.

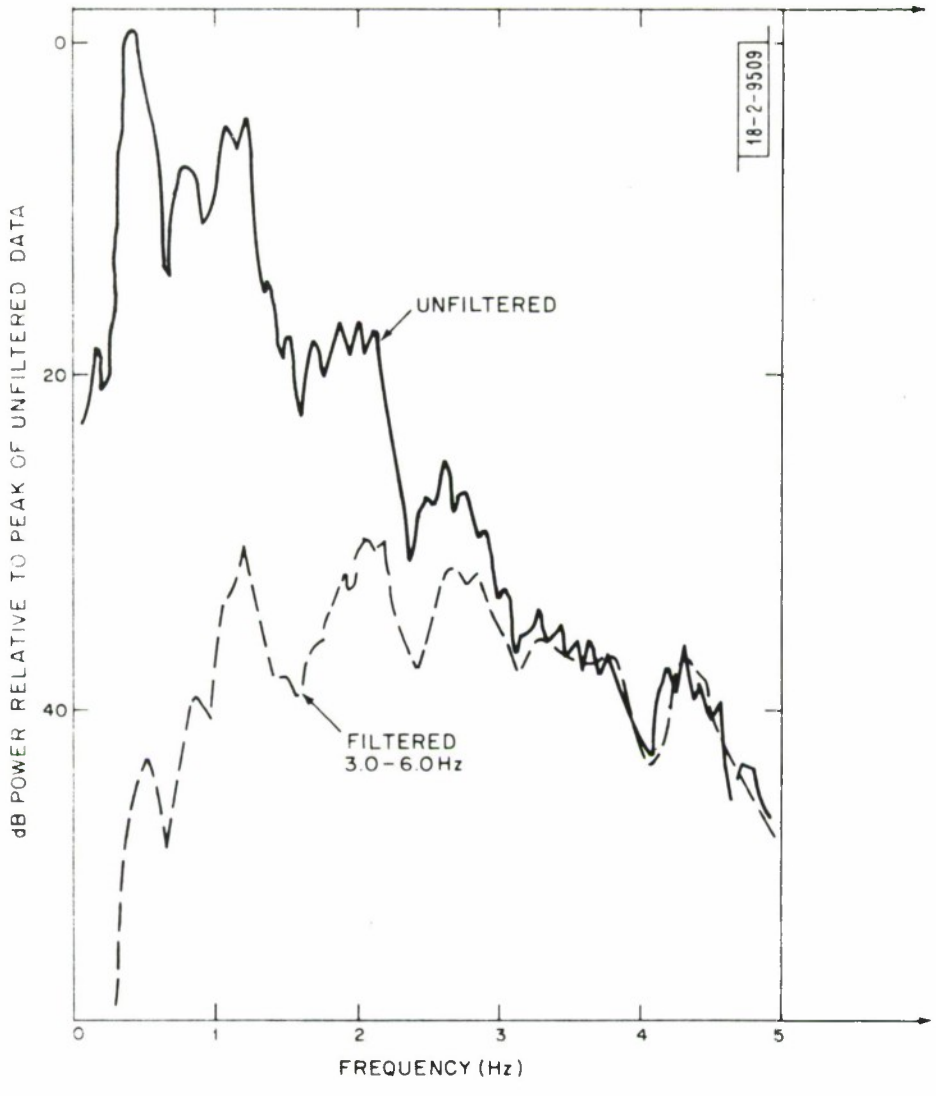

(b) Earthquake.

Fig. 9. Continued.

VI. SPECTRAFORMING AS A SIGNAL PROCESSING METHOD FOR DISCRIMINATION

We have thus far discussed large array signal processing of large events with no consideration of the purpose of the signal processing. The large arrays have been constructed to aid in the detection and identification of underground nuclear explosions and it has been demonstrated, usually using beams formed from subarray sums, that many events can be correctly identified as earthquakes or explosions by the spectral shape in the short period band. Briefly, for a given body wave magnitude the explosions tend to generate relatively more high frequency energy than the earthquakes. This observation was made using beams of straight sums so the spectra considered were on the average given by our equation (26) where S is somehow the intrinsic event spectrum. The other factors are unknown. If straight sums were replaced by steered subarrays then the output quantity would be larger for a given $|S|^2$. Also, the differences between event types would be somewhat larger. Finally consider the average spectrum of all of the sensors. We shall call this spectraforming. On the average, for a given $|S|^2$ this has the largest output of all and the differences between event types should also be largest. Thus, in the absence of background noise, it would seem that spectraforming may be superior to beamforming for discrimination based upon short period spectra. Note that this does not mean that the spectraform is a better or worse estimate of $|S|$ than is the spectrum of the beam. It is just different.

Unfortunately spectraforming does not reject additive background noise as well as does beamforming. This is true even when corrections are made to remove the average contribution of the noise. From this point of view beamforming is a superior processing method since it can look further down into the noise. In the remainder of this report we consider the trade off between noise reduction and signal related power

for different processing methods. We shall see that there are conditions when spectra-forming is definitely the superior processing method for discrimination.

The notation of the preceding sections is somewhat cumbersome for some of the analysis to be done in the sequal. We therefore will introduce a notation which does not specify the signal structure so completely. Let K = NM where N is the number of subarrays and M is elements per subarray. Let all sensors be singly indexed and let S_k be the spectrum of the signal on the kth sensor. Thus S_{mn} has been replaced by S_k in our notation. If Y_i is the transform of the zero mean additive noise on sensor i then

$$X_i(f) = S_i(f) + Y_i(f) \tag{39}$$

is the actual spectrum observed at sensor i. In this case we assume the data interval is fixed so all these quantities are finite. We assume noise at different sensors is independent. For sensor spacings of three kilometers this is a good approximation for frequencies greater than 0.7 Hz. Larger separations are required at lower frequencies. We also assume that the real and imaginary parts of Y_i are independent, that $Y_i(f)$ has zero mean, that

$$E\, Y_i(f) Y_i^*(f) = 2\sigma_Y^2(f), \tag{40}$$

and that Y_i is independent of S_j for any i, j. We also assume there exists a set of L complex random variables, Z_i, i = 1, . . L which have the same distribution as Y_i but are independent of each other and of all the Y_i and S_i. These Z_i could be transforms of blocks of noise preceding the event arrival time and will be used to correct spectra-forming and beamforming spectra for average noise effects.

The spectraform power estimator which we will study is

$$\hat{P}(f) = \frac{1}{K}\left(\sum_{k=1}^{K} X_i(f)X_i^*(f)\right) - \frac{1}{L}\left(\sum_{\ell=1}^{L} Z_i Z_i^*\right) . \tag{41}$$

The last term on the right is a correction introduced so that given the S_i the expected value of $\hat{P}(f)$ is what it would be with $\sigma_Y = 0$. In this sense $\hat{P}(f)$ is unbiased. The beam estimator for power is

$$\hat{P}_B(f) = \left|\frac{1}{K}\sum_{k=1}^{K} X_k(f)\right|^2 - \frac{1}{KL}\left(\sum_{\ell=1}^{L} Z_\ell Z_\ell^*\right) . \tag{42}$$

The last term is again a correction introduced so that given the S_i the expected value of $\hat{P}_B(f)$ is the value with no noise present. This correction term makes it convenient to compare the value of $\hat{P}_B$ and $\hat{P}$ for discrimination on the basis of their stability. That is, since both P_B and P are unbiased estimates, the one with the smaller standard deviation relative to its expected value is more desirable for discrimination. Note that $E\{\hat{P}_B | S_k, k=1, \ldots K\} \neq E\{\hat{P} | S_k, k=1, \ldots K\}$ except if all the S_i are equal.

In this report we deal only with $\hat{P}$ and $\hat{P}_B$ conditioned on the values of S_k, k=1, . . . K. Thus quantities such as the expected value of $\hat{P}$ and $(\hat{P})^2$ are conditional. Ultimately we must take expectations over the S_k. This appears to be feasible but has not yet been accomplished. It will require that the distribution of the S_k be specified or at least all moments up to the fourth be given.

VII. CONDITIONAL MOMENTS AND STABILITY OF $\hat{P}_B$ AND $\hat{P}$

The average power from all channels in the absence of noise is

$$P(f) = \frac{1}{K} \sum_{k=1}^{K} S_k(f) S_k^*(f). \tag{43}$$

and the power of the average of the channels is

$$P_B(f) = \left| \frac{1}{K} \sum_{k=1}^{K} S_k(f) \right|^2 \tag{44}$$

These are the same as equations (6) and (8) with the notation slightly changed. It is easy to see that the expected value of $\hat{P}$ given P is

$$E(\hat{P} \mid P) = P. \tag{45}$$

and is the same as $E\{\hat{P} \mid S_k, k=1 \ldots K\}$. This comes from expanding $\hat{P}$,

$$\hat{P} = \frac{1}{K} \sum_{k=1}^{K} S_k S_k^* + \frac{1}{K} \sum_{k=1}^{K} S_k Y_k^* + \frac{1}{K} \sum_{k=1}^{K} S_k^* Y_k + \frac{1}{K} \sum_{k=1}^{K} Y_k Y_k^* - \frac{1}{L} \sum_{\ell=1}^{L} Z_\ell Z_\ell^*, \tag{46}$$

and taking the conditional expected value

$$E(\hat{P} \mid P) = P + 0 + 0 + 2\sigma_Y^2 - 2\sigma_Y^2. \tag{47}$$

Although this expected value is taken conditioned on all the S_k it happens that the S_k enter the result only as P. Similarly

$$\hat{P}_B = \frac{1}{K^2} \left(\sum_{k=1}^{K} \sum_{k'=1}^{K} S_k S_{k'}^* + S_k Y_{k'}^* + S_k^* Y_{k'} + Y_k Y_{k'}^* \right) - \frac{1}{KL} \sum_{\ell=1}^{L} (Z_\ell Z_\ell^*) \tag{48}$$

and taking expectations,

$$E(\hat{P}_B \mid P_B) = P_B + 0 + 0 + \frac{2\sigma_Y^2}{K} - \frac{2\sigma_Y^2}{K} = P_B \tag{49}$$

and $$E(\hat{P}_B \mid P_B) = E(\hat{P}_B \mid S_k,\ k = 1, \ldots K).$$

The conditional expectation $E(\hat{P}^2 \mid P) = E(\hat{P}^2 \mid S_k, k = 1 \ldots K)$ can be obtained by squaring (46) and using the fact that several of the resulting terms have zero expected values, given the S_i. For example the expected value of any term which is third order in Y_k, Y_k^*, Z_k or Z_k^* has zero expected value due to the symmetry of the assumed distributions. Also $EY_kY_k = EY_k^*Y_k^* = EZ_kZ_k = EZ_k^*Z_k^* = 0$ since the amplitude and phase of Y_k (or Z_k) are independent and the phase is uniformly distributed over 2π. The result is

$$E(\hat{P}^2 \mid P) = P^2 + \frac{2P}{K}(2\sigma_Y^2) + E\left(\frac{1}{K}\sum_{k=1}^{K} Y_kY_k^*\right)^2 - 8\sigma_Y^4 + E\left(\frac{1}{L}\sum_{\ell=1}^{L} Z_\ell Z_\ell^*\right)^2 . \tag{50}$$

But

$$E\left(\frac{1}{K}\sum_{k=1}^{K} Y_kY_k^*\right)^2 = (E(Y_kY_k^*))^2 - \frac{(E(Y_kY_k^*))^2}{K} + \frac{(E(Y_kY_k^*)^2)}{K} \tag{51}$$

and, because Y_k is complex Gaussian, it can be shown that

$$E(Y_kY_k^*)^2 = 8\sigma_Y^4 . \tag{52}$$

Thus

$$E\left(\frac{1}{K}\sum_{k=1}^{K} Y_kY_k^*\right)^2 = 4\sigma_Y^4\left(1 + \frac{1}{K}\right) \tag{53}$$

and similarly

$$E\left|\frac{1}{L}\sum_{\ell=1}^{L} Z_\ell Z_\ell^*\right|^2 = 4\sigma_Y^4\ (1+\frac{1}{L})\ . \tag{54}$$

Substituting back gives

$$E(\hat{P}^2 \mid P) = P^2 + \frac{4\sigma_Y^2 P}{K} + \frac{4\sigma_Y^4}{K}(1+\frac{K}{L}) \tag{55}$$

Finally, to obtain $E(\hat{P}_B^2 \mid P_B) = E(\hat{P}_B^2 \mid S_k,\ k=1, \ldots K)$ we recall that

$$S_B = \frac{1}{K}\sum_{k=1}^{K} S_k, \tag{56}$$

which is equation (8) in new notation, and define

$$y = \frac{1}{K}\sum_{k=1}^{K} Y_k\ . \tag{57}$$

The variable y is zero mean Gaussian with

$$E\ yy^* = \frac{2\sigma_Y^2}{K}\ . \tag{58}$$

We can now express $\hat{P}_B$, defined by equation (42), as

$$\hat{P}_B = |S_B + y|^2 - \frac{1}{KL}\sum_{\ell=1}^{L} Z_\ell Z_\ell^*\ . \tag{59}$$

Squaring this and taking expected values gives

$$E(\hat{P}_B^2 \mid P_B) = P_B^2 + 2P_B\frac{2\sigma_Y^2}{K} + E|yy^*|^2 - \frac{8\sigma_Y^4}{K^2} + \frac{1}{K^2}\ E\left|\frac{1}{L}\sum_{\ell=1}^{L} Z_\ell Z_\ell^*\right|^2. \tag{60}$$

But

$$E|yy^*|^2 = \frac{8\sigma_Y^4}{K^2} \tag{61}$$

and

$$E\left\{\frac{1}{L}\sum_{\ell=1}^{L} Z_\ell Z_\ell^*\right\}^2 = 4\sigma_Y^4\left(1+\frac{1}{L}\right) \tag{62}$$

so that

$$E(\hat{P}_B^2 \mid P_B) = P_B^2 + \frac{4\sigma_Y^2 P_B}{K} + \frac{4\sigma_Y^4}{K^2}\left(1+\frac{1}{L}\right) \tag{63}$$

It is now simple to obtain conditional variances of P and P_B from equations (45), (49), (55), and (63). These are

$$E\{(\hat{P}-P)^2 \mid P\} = \frac{4\sigma_Y^4}{K}\left(\frac{P}{\sigma_Y^2}+\left(1+\frac{K}{L}\right)\right) \tag{64}$$

and

$$E\{(\hat{P}_B - P_B)^2 \mid P_B\} = \frac{4\sigma_Y^4}{K}\left(\frac{P_B}{\sigma_Y^2}+\frac{1}{K}\left(1+\frac{1}{L}\right)\right). \tag{65}$$

The quality of estimates of quantities such as power spectra is often measured by the stability of the estimate. The stability is the ratio of the square of the expected value to the variance. Intuitively it is clear that large stability means that the estimate is usually near to its mean value and, if the estimate is unbiased, near to the true value of the quantity being estimated. When the estimate has a χ^2 distribution or if it can be approximated by a χ^2 then the degrees of freedom is twice the stability and this can be used to generate confidence intervals. For example, if stability is 2 for a χ^2 variable then in the long run 80% of the observations will be in the interval from 0.26 to 1.94 times the expected value. If stability is increased to 4 then 80% of the time it will be in the interval 0.43 to 1.67 times the expected value.

The stability for spectraforms is obtained from preceding relations and is

$$s = \frac{[E\{\hat{P} \mid P\}]^2}{E\{(\hat{P}-P)^2 \mid P\}} = \frac{P^2}{\frac{4\sigma_Y^4}{K}\left(\frac{P}{\sigma_Y^2} + (1 + \frac{K}{L})\right)} \tag{66}$$

We define the quantity

$$r = \frac{P}{\sigma_Y^2} \tag{67}$$

which is equal to twice the ratio of expected signal power to expected noise power on a single sensor. That is, it is twice the signal to noise ratio on a single sensor. Using this

$$s = \frac{Kr^2}{4\,(r + (1 + \frac{K}{L}))} \tag{68}$$

The stability of the beamform power is

$$s_B = \frac{P_B^2}{\frac{4\sigma_Y^4}{K}\left(\frac{P_B}{\sigma_Y^2} + \frac{1}{K}(1 + \frac{1}{L})\right)} \tag{69}$$

Using the definition

$$g \equiv P/P_B \tag{70}$$

this becomes

$$s_B = \frac{\left(\frac{Kr}{g}\right)^2}{4\left(\frac{Kr}{g} + (1 + \frac{1}{L})\right)} \tag{71}$$

The expression

$$r_B \equiv \frac{Kr}{g} \tag{72}$$

can be recognized as twice the signal to noise ratio on the beam of K sensors.

It is somewhat intuitive but reasonable to assert that an unbiased estimate with greater stability will be superior for discrimination purposes. We therefore compare $\hat{P}$ and $\hat{P}_B$ on that basis. For this purpose it is convenient to assume $L = \infty$. This is not essential but does remove one variable whose effect, in principle, can be made vanishingly small. In this case s will be larger than s_B if

$$K \geq g^2 / (r + 1 - rg). \tag{73}$$

Figure 10 shows the region of K,g plane where beamforming is less stable for several different values of r. Given K and r one can determine the minimum g which will make spectraforming the superior procedure. One can then judge from equation (35) and others of previous sections if it is reasonable to anticipate a value of g which will be larger than this. Of course this approach assumes, incorrectly, that P and P_B always achieve their expected value. Consideration of the more realistic case when P and P_B are treated completely as random variables is defered to a future report.

It is not satisfactory to know which of the processing methods is superior but it is important to know if either is actually satisfactory. For example, if beamforming is superior to spectraforming for some set of parameters but it has stability 0.1 it is not likely that the measurement can be of much value for discrimination purposes. To determine if an estimator might be satisfactory we must actually consider its stability. Figures 11 and 12 show the stability achieved by beamforming and spectraforming as a function of various parameters. In the case of beamforming the stability is a simple function of the signal to noise parameter $r_B = Kr/g$. For spectraforming the stability is a function of K and r independently and has been shown as a contour map of s.

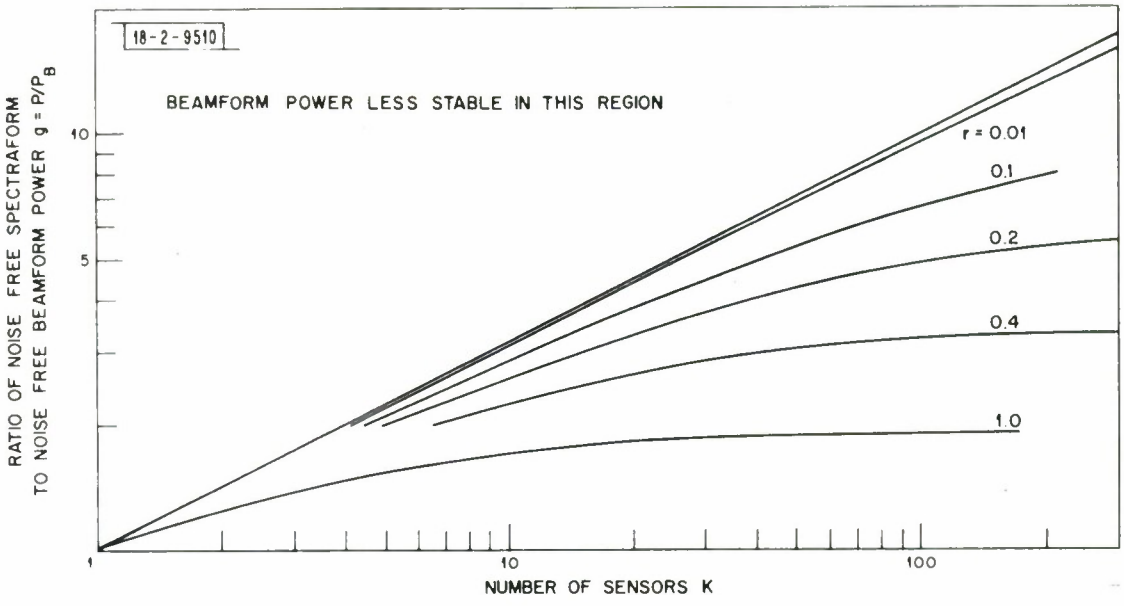

Fig. 10. Conditions for spectraform power estimates to be more stable than beamform power. Noise spectrum known, beampower = P_B, spectraform power = $P = gP_B$.

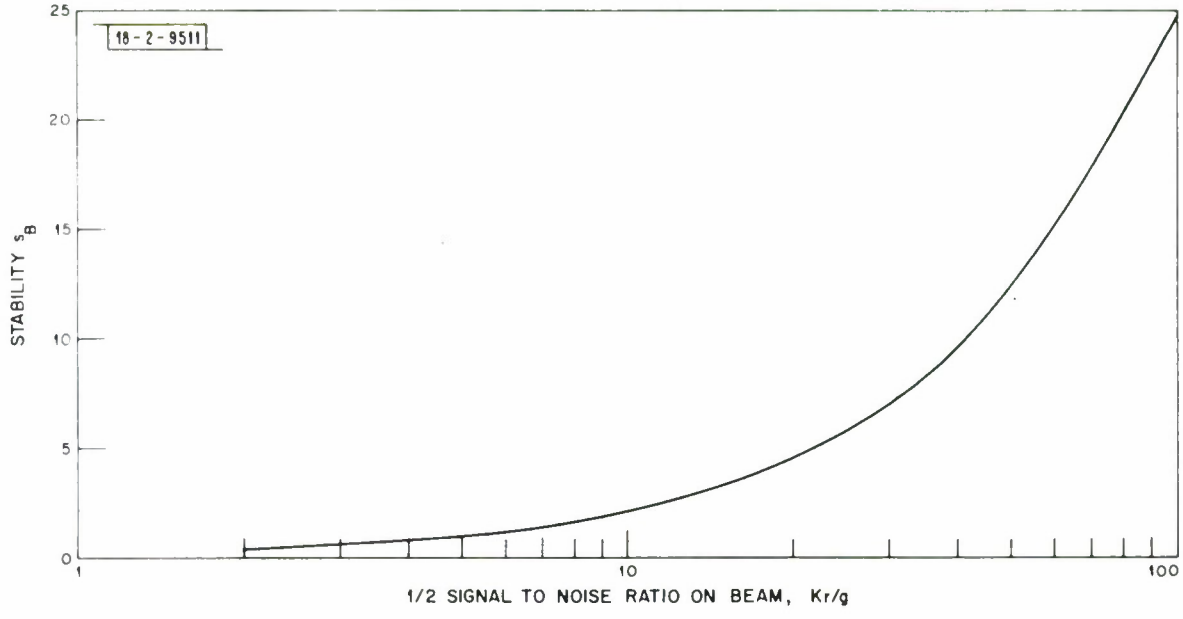

Fig. 11. Stability of beamform power estimate vs 1/2 (signal to noise ratio on the beam).

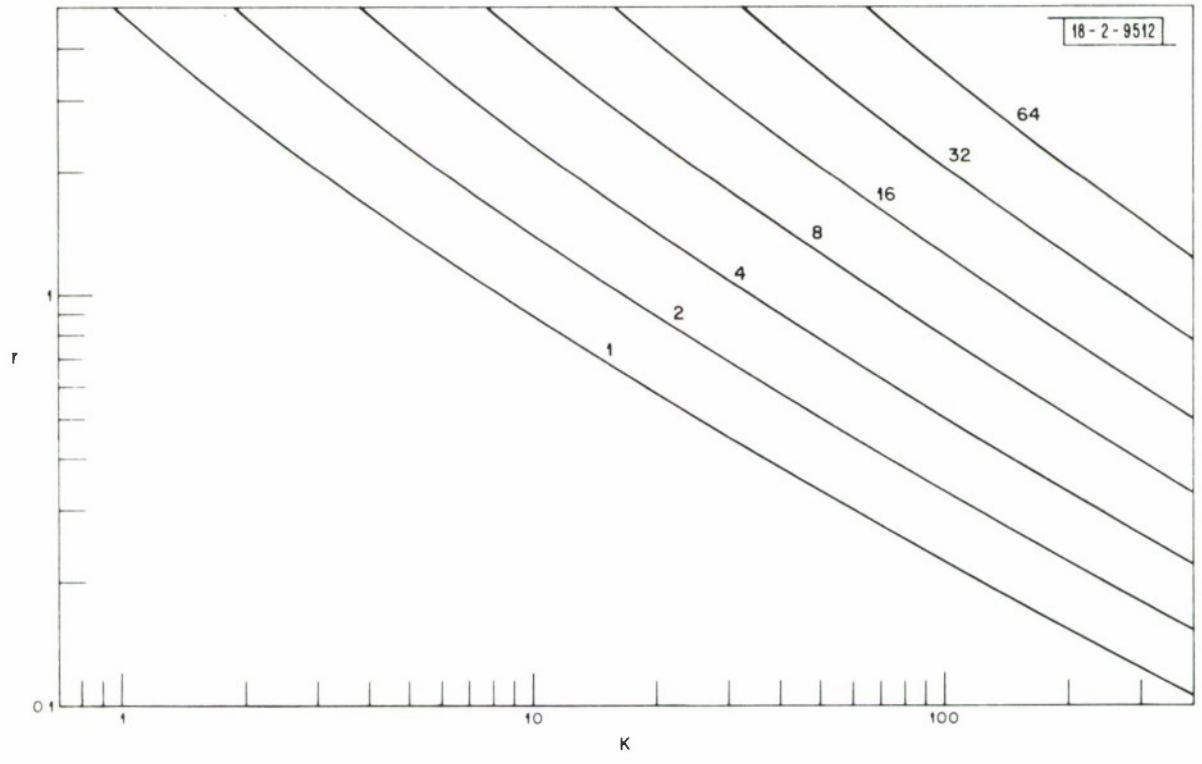

Fig. 12. Stability of spectraform as a function of number of sensors, K, and 1/2 (signal to noise ratio on a single sensor), r.

Examples were given previously of the 80% confidence intervals of χ^2 random variables with stabilities of 2 and 4. We shall continue our discussion utilizing these two values as marginally acceptable stability values for a spectral estimate which might be applied for discrimination. This decision is somewhat arbitrary. Our further discussions could be continued with other values of stability and the specific results would be changed. It is hoped that minimum stabilities of 2 or 4 represent realistic limits and thus lead to correct conclusions.

We now also limit the discussion to K=210 (corresponding to 10 sensors from each of the 21 LASA subarrays) and K=21 (one sensor from each subarray). These restrictions allow us to reach specific conclusions about reasonably interesting specific cases and at the same time demonstrate the analysis which could be done for any specific case of interest.

Consider the case of 10 sensors from each of 21 subarrays. From Figure 12 or equation (68) we see that $r \geq 0.22$ assures $s \geq 2$ and $r \geq .32$ for $s \geq 4$. From Figure 11 or equation (71) we observe that $Kr/g \geq 8.9$ assures $s_B \geq 2$ and $Kr/g \geq 17$ for $s_B \geq 4$ so, with K=210, we have $r/g \geq 0.042$, and $r/g \geq 0.081$ respectively. Now, assuming that g behaves as $E\{P|S,T\}/E\{P_B|S,T\}$, which was determined for LASA as a function of frequency in an earlier section, we can determine that value of r which is required to give satisfactory stability for a beamforming power spectral estimate. Figure 7 showed g in dB for the case at hand. It has been redrawn on a linear scale on Figure 13. We now note that if $r < 0.22$ and $f > 1.6$ Hz then $r/g < 0.042$. Thus if $f > 1.6$ Hz then spectraforming can achieve stability 2 with $r = 0.22$ but beamforming requires a larger signal to noise factor. In that sense spectraforming will be superior to beamforming for $f > 1.6$Hz if a stability factor of 2 is satisfactory. If a stability factor of 4 is re-

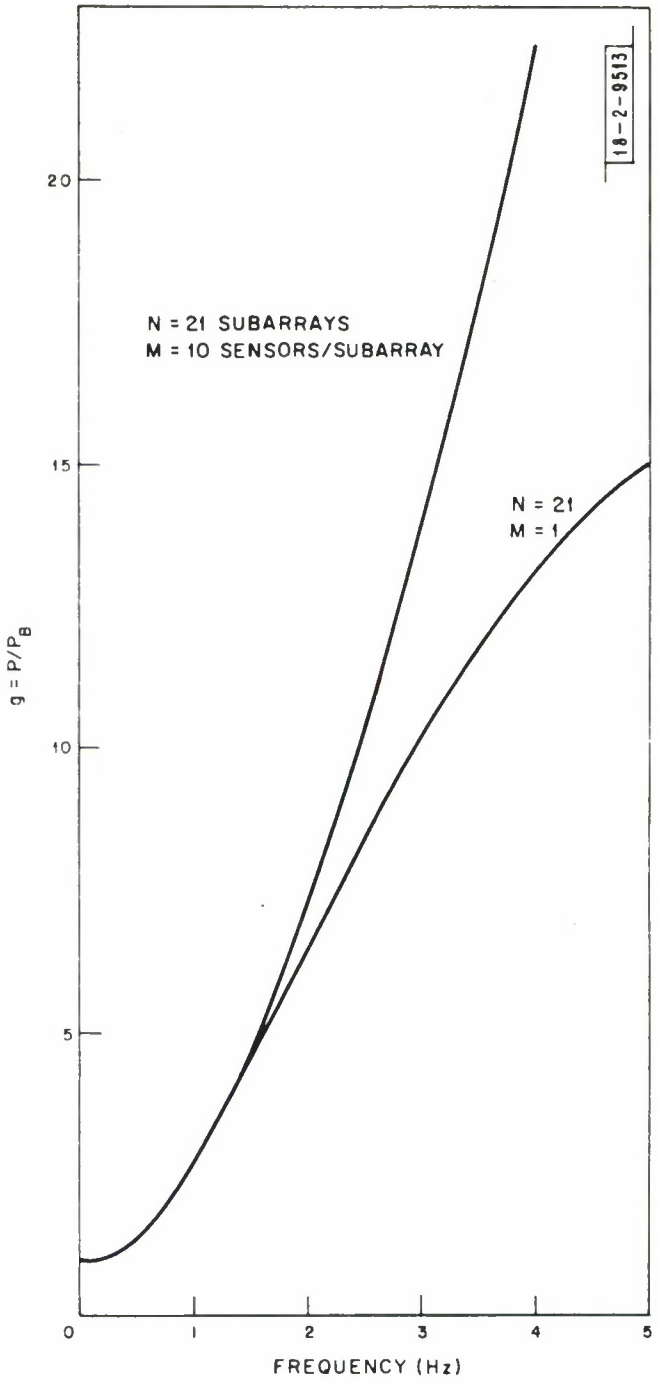

Fig. 13. Ratio of expected spectraform signal power to expected beamform signal power vs frequency. $\sigma = f$, $\sigma_S = 0.3f$.

quired then spectraforming will achieve it with $r \geq 0.32$ and will be superior to beamforming if $f \geq 1.3$ Hz. In either case if we are in the region of spectraforming superiority then this cannot be changed by increasing r. This is clear from Figure 10 since increasing r causes the separation lines to be even lower on the figure.

Now suppose only one sensor is used from each subarray. Nominal g for LASA has been shown on Figure 13. Using this we determine that spectraforming will be superior for $f \geq 1.7$ Hz if a stability of 2 is satisfactory and $f \geq 1.3$ if a stability of 4 is required.

The preceding discussion has dealt with spectraforming and beamforming. It is a simple matter to use the same methods to compare spectraforming and beams made from subarray straight sums. The only difference is that g(f) is changed and is larger by the amount indicated by the curves on Figure 7. Thus for beamforming of subarray sums spectraforming will become the superior method at even lower frequencies. For example, g at $f = 1.2$ is about what it was at $f = 1.6$ for beamforming 210 individual sensors. This means that if a stability of 2 is satisfactory then spectraforming will be superior for $f \geq 1.2$. Similarly if stability 4 is required $f \geq 1.05$ will make spectraforming superior.

The impact of using reasonable but less than perfect estimates of the noise spectra ($L \neq \infty$) could be included in the above discussion. This would not change the general conclusion that, as frequency increased, spectraforming becomes the superior processing method some place in the range $1.0 \leq f \leq 2.0$ Hz.

VIII. OBSERVED SIGNAL TO NOISE RATIOS

In the previous section we discussed signal processing as a function of r, which is twice the signal to noise ratio on a single sensor. It is of interest to know what values of r might be achieved for events of different magnitudes. This would allow one, for example, to determine the lowest magnitude for which meaningful data at some frequency, f, might be obtained. We briefly discuss this in this section. The data are limited and are at best only roughly indicative of what might be obtained for a large number of events. Some points ignored include possible variation of spectral shape with magnitude, time variations in noise levels, actual achievable stability in noise power estimates, and the fact that the actual use of the data might change stability requirements considerably. We consider only the case of 21 subarrays of 10 sensors and assume that a stability factor of 2 is satisfactory. Thus, for high frequencies, we wish to know at what magnitude we obtain $r \leq 0.22$ which is equivalent to a signal to noise ratio less than or equal to -9.6 dB. We do not discuss performance below about 1.0 Hz where beamforming or optimal linear combining will yield results superior to spectraforming.

Figure 14 shows spectra for the two large events we have used previously. The noise spectra were obtained as the average power of 21 sensors for a 10 second interval just before the event. The average power on the same sensors is shown for the event plus noise interval. The difference in dB is also shown on the figure. If the noise spectrum is many dB down from the sum of signal and noise then the signal plus noise spectrum is essentially the signal spectrum. Thus for both of these events the signal plus noise to noise ratio can be taken as the signal to noise ratio. Clearly there is no signal to noise problem for either of these events in the range 1.0 to 5.0 Hz.

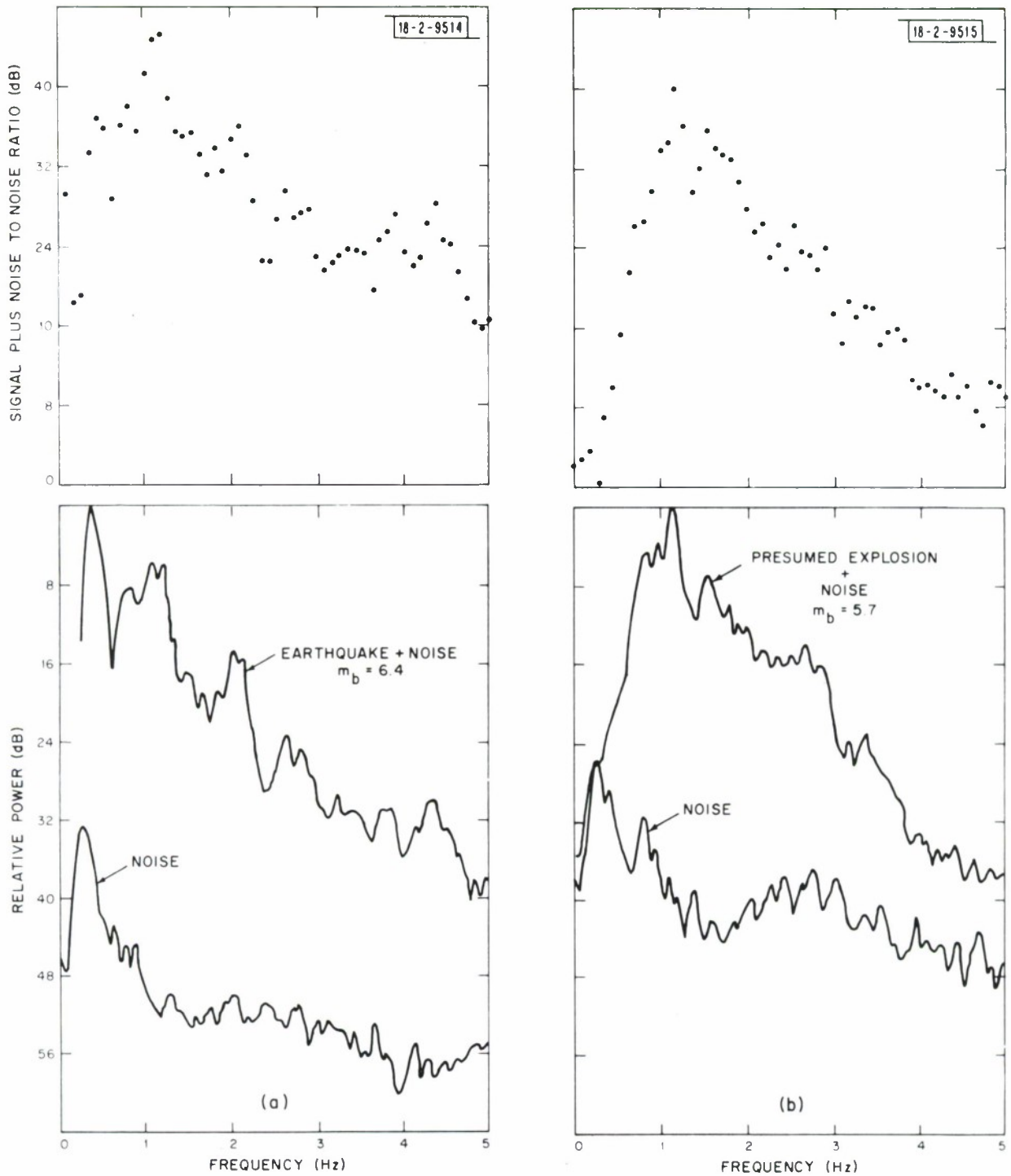

Fig. 14. Spectra of noise and of signal plus noise. (a) Earthquake with $m_b = 6.4$. (b) Presumed explosion with $m_b = 5.7$.

Suppose we are interested in using event spectra up to 3.0 Hz. At this frequency we can use the data if spectraforming is done and the signal to noise ratio is at least -9.6 dB. At 3.0 Hz the earthquake and explosion at hand have signal to noise ratios of about 25 and 20 dB respectively. This means that the signal power could be reduced by about 35 and 30 dB respectively and still give a stability factor of 2. But 35 and 30 dB are equivalent to 1.75 and 1.5 magnitude units if event sizes are scaled with no spectral changes. Thus we would expect to get useful data up to 3 Hz for an earthquake with $m_b \geq 4.65$ and an explosion with $m_b \geq 4.2$. At 2.0 Hz the SNR is 8 to 10 dB higher so data should be useful for events another 0.5 magnitude units smaller.

Data similar to that on Figure 14 has been obtained for two somewhat smaller events and is shown on Figure 15. It appears that the SNR at 3 Hz is about 10 dB for the presumed explosion and (perhaps optimistically) -3 dB for the earthquake. This implies we can operate down to $m_b \simeq 4.2$ for explosions and $m_b \simeq 4.8$ for earthquakes. Those numbers are in suprisingly good agreement with those above considering all of the random factors involved. Again at 2.0 Hz these figures can be reduced by 0.5 magnitude units or more.

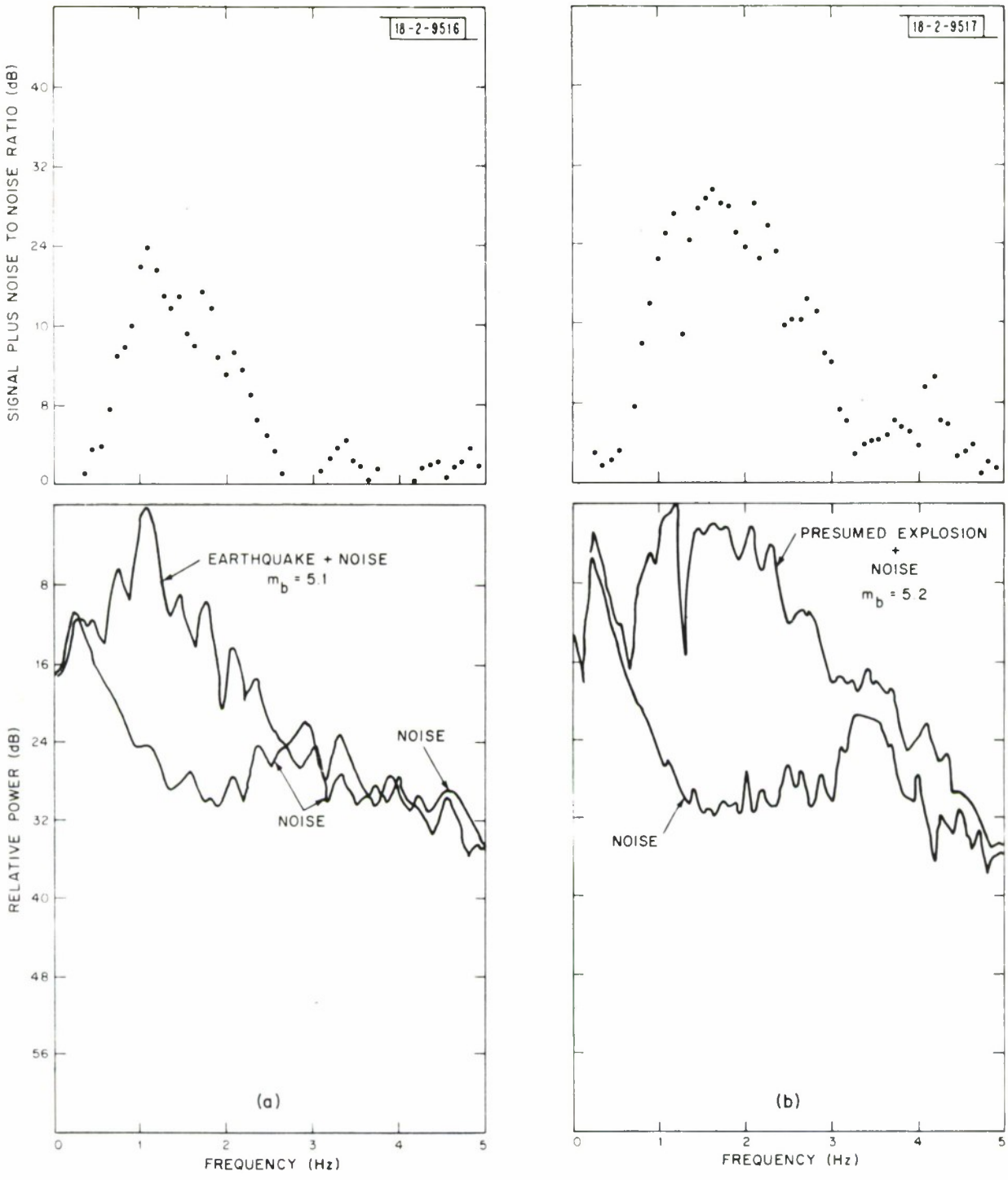

Fig. 15. Spectra of noise and of signal plus noise. (a) Earthquake with $m_b = 5.1$. (b) Presumed explosion with $m_b = 5.2$.

IX. DISCUSSION AND CONCLUSION

The theoretical analysis and the data we have discussed suggest that it is possible to obtain useful spectral information for teleseismic P-waves at frequencies as large as 3.0 Hz for events in the range $4.0 \leq m_b \leq 4.5$. This assumes that spectraforming is done to obtain spectra for frequencies above, say, 1.0 Hz. The choice of spectraforming even down to 1.0 Hz and somewhat below is acceptable since if spectraforming gives satisfactory spectra in the range 2.0 to 3.0 Hz it will also in the 1.0 to 2.0 Hz range because the SNR is much higher there. Spectraforming will be less successful much below 1.0 Hz since signal variations between sensors will not be very large. In that case the noise rejection power of beamforming or some other linear processing method would probably give a significant advantage over spectraforms. Of course one must recall the problem that at frequencies of 0.2 to 0.5 Hz the noise is not independent between sensors so beamforming cannot normally achieve as much noise reduction as at higher frequencies. In general in this report we have not considered alternative signal processing methods at these lower frequencies.

In many respects the material in this report is exploratory and preliminary. As such it leaves several partially explored areas for further development. We conclude this report by mentioning some of the remaining research which might be undertaken.

A statistical model for the generation of seismic signal variations has been suggested and partially analyzed. This model should be investigated further. This should include inquiries into the physical source of signal variations as well as more statistical analysis. For example the physics should be used to help choose the frequency dependence of parameters such as $\sigma^2(f)$ and the form of the distribution of the $\mathcal{H}_{mn}$. Once the distribution of the $\mathcal{H}_{mn}$ is fixed, perhaps log normal as suggested in the introduc-

tion, then the theoretical comparison of alternative processing schemes can be completed.

Spectraforming can be used to obtain spectra at high frequencies even for relatively small teleseismic events. However, these same events may cause difficulties in the low frequency band from, say, 0.2 to 0.8 Hz. If one wishes to obtain meaningful spectral information over as wide a band as possible, even for small events, then methods for obtaining improved spectral estimates in this low frequency band should be carefully considered. It may be a crucial region for discrimination.

Suppose that reasonably stable estimates of event power as a function of frequency can be obtained in the range from 0.3 to 3.0 Hz even for events in the magnitude range $4.0 \leq m_b \leq 4.5$. The potential utilization of such data for discrimination should be more thoroughly investigated than it has in the past. Discriminants should, if possible, be based upon differences which can be predicted using theoretical models of earthquake and explosion signal generation. Discriminants not supported by a theoretical model and carefully tailored to available data should be avoided if possible.

Finally, when it has been determined how relatively broadband short period spectral information might be used for discrimination in the 4.0 to 4.5 body wave magnitude range the specific proposed method must be tested with a nontrivial quantity of data. The specific signal processing methods and discrimination rules must be identified and such a test conducted. This assumes that a procedure potentially superior to beamforming of subarray straight sums and using the Lincoln Laboratory spectral ratio with those beams can be found.

DOCUMENT CONTROL DATA – R&D

(Security classification of title, body of abstract and indexing annotation must be entered when the overall report is classified)

1. ORIGINATING ACTIVITY *(Corporate author)* Lincoln Laboratory, M.I.T.	2a. REPORT SECURITY CLASSIFICATION Unclassified 2b. GROUP None

3. REPORT TITLE

Processing a Partially Coherent Large Seismic Array for Discrimination

4. DESCRIPTIVE NOTES *(Type of report and inclusive dates)*
Technical Note

5. AUTHOR(S) *(Last name, first name, initial)*

Lacoss, Richard T. and Kuster, Guy T.

6. REPORT DATE	7a. TOTAL NO. OF PAGES	7b. NO. OF REFS
27 November 1970	52	None

8a. CONTRACT OR GRANT NO. F19628-70-C-0230 b. PROJECT NO. ARPA Order 512 c. d.	9a. ORIGINATOR'S REPORT NUMBER(S) Technical Note 1970-30 9b. OTHER REPORT NO(S) *(Any other numbers that may be assigned this report)* ESD-TR-70-353

10. AVAILABILITY/LIMITATION NOTICES

This document has been approved for public release and sale; its distribution is unlimited.

11. SUPPLEMENTARY NOTES	12. SPONSORING MILITARY ACTIVITY
None	Advanced Research Projects Agency, Department of Defense

13. ABSTRACT

A stochastic model has been proposed to characterize the teleseismic short period P-wave signal variations observed within a Large Aperture Seismic Array (LASA). The model asserts that, in the frequency domain, the received signal is equal to some average signal multiplied by a random gain and phase. Within a Montana LASA subarray the mean value of the modulus squared of the random term can be roughly approximated by $1 + 0.18f^2$, where f is frequency. For sensors drawn from the full LASA aperture the value is approximated by $1 + 2.0f^2$.

An incoherent signal processing method, spectraforming, is introduced as a viable alternative to beamforming for obtaining spectral information at frequencies above about 1.0 Hz. The spectraform is essentially the average power in sensors with a correction subtracted for background noise power contributions. It is demonstrated that, although beamforming will give more noise rejection than spectraforming, the latter can be superior in terms of output signal to noise ratio when input signal variations between sensors are large.

Expressions have been obtained for the signal power spectral density expected from various modes of processing. Spectra from subarray beams and sums, spectra from array beams and beams of subarray sums, and spectraforms are all considered. Results show for example that the event power output from spectraforming, beamforming of individual sensors, and beamforming of subarray sums will decrease in that order. In the case of actual events considered the amounts of loss at 3.0 Hz, relative to spectraforming, are about 10 and 20 dB, respectively.

14. KEY WORDS

LASA seismometers spectraforming